Journal Pre-proof

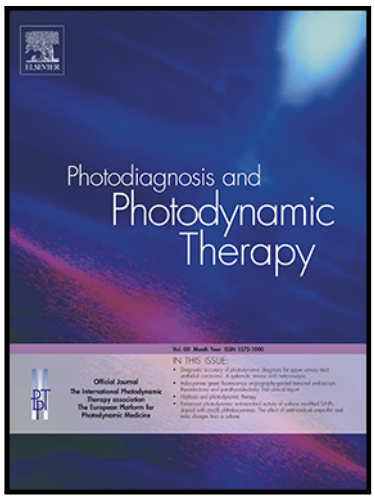

Clinical Features Evaluation of Myopic Fundus tessellation from OCTA and MfERG

Yanyan Zhang , Yan Zhong , Wei Mao , Zhe Zhang , Yusheng Zhou , Hu Li , Jianing Ying , Quanyong Yi

PII: S1572-1000(25)00023-7
DOI: https://doi.org/10.1016/j.pdpdt.2025.104493
Reference: PDPDT 104493

To appear in: *Photodiagnosis and Photodynamic Therapy*

Received date: 10 November 2024
Revised date: 20 January 2025
Accepted date: 21 January 2025

Please cite this article as: Yanyan Zhang , Yan Zhong , Wei Mao , Zhe Zhang , Yusheng Zhou , Hu Li , Jianing Ying , Quanyong Yi , Clinical Features Evaluation of Myopic Fundus tessellation from OCTA and MfERG, *Photodiagnosis and Photodynamic Therapy* (2025), doi: https://doi.org/10.1016/j.pdpdt.2025.104493

Highlight

- OCTA and MfERGwas used to comprehensively analysed the morphology, function and blood flow in myopic FT, providing new insights for research on pathologic myopia.
- As the severity of myopic tessellated fundus increases, the subfoveal choroidal thickness decreases, and the amplitudes of N1 and P1 waves in multifocal electroretinography reduce, with an elongation in their latency periods.
- When SFCT thins, the amplitudes and latency periods of N1 and P1 waves also change.
- The assessment of tessellated fundus changes may guide clinical treatment and the early management of pathologic myopia.

Clinical Features Evaluation of Myopic Fundus tessellation from OCTA and MfERG

Yanyan Zhang[1], Yan Zhong[2]*, Wei Mao[1], Zhe Zhang[1], Yusheng Zhou[1], Hu Li[1], Jianing Ying[1#], Quanyong Yi[1#].*

[1]Ningbo Eye Hospital, Wenzhou Medical University, Ningbo, Zhejiang 315000, P.R. China.

[2]The First Affiliated Hospital of Ningbo University, Ningbo, Zhejiang 315000, P.R. China.

Correspondence to:

Quanyong Yi, Ningbo Eye Hospital, Wenzhou Medical University, Ningbo, Zhejiang 315000, P.R. China. E-mail: yiquanyongteam@163.com.

Jianing Ying, Ningbo Eye Hospital, Wenzhou Medical University, Ningbo, Zhejiang 315000, P.R. China. E-mail: 2662431632@qq.com.

Authors' email address:

Yanyan Zhang: zyyeyedoctor@163.com, Yan Zhong: 593908615@qq.com, Wei Mao: fushaoying@126.com, Zhe Zhang: pengbo0451 @163.com, Yusheng Zhou: 103690@qq.com, Hu Li: tigerle333@163.com, Jianing Ying: 2662431632@qq.com, Quanyong Yi: yiquanyongteam@163.com.

Author contributions

Each author has made a contribution. *****These authors contributed equally contributed equally as co-first authors. [#]These authors contributed equally as co-corresponding authors. YYZ and YZ wrote the manuscript and revised it critically for important intellectual content. WM and ZZ: Data analysis and collation. YSZ

and HL: Formulation and evaluation of the experimental scheme. JNY : Revise the paper. YQY: Design the study.

Foundation item

This work was supported by Ningbo Medical Science and Technology Project (2021Y57), Ningbo Yinzhou District Agricultural Community Development Science and Technology Project (2022AS022). Ningbo Eye Hospital Science and Technology Project (2023YB004), Ningbo Eye Hospital Talent Project (2022RC001).

Data availability statements

The datasets used and/ or analyzed during the present study are available from the corresponding author on reasonable request.

Ethics statement

The Medical Research Ethics Committee of Ningbo Eye Hospital (No. 2023022). **Competing interests**

This study did not receive any industrial support. The authors have no competing interests to declare regarding this study.

ABSTRACT

Purpose: To evaluate the differences in fundus tessellation among various severities using multifocal visual electrophysiology (MfERG) and optical coherence tomography angiography (OCTA) for clinical grading and treatment.

Methods: This study included 52 patients totaling 87 eyes. The Early Treatment Diabetic Retinopathy Study (ETDRS) grid division method was utilized to assess Grade of fundus tessellation. Data obtained via OCTA and ImageJ software included macular foveal thickness (MT), subfoveal choroidal thickness (SFCT), superficial retinal capillary layer vascular density (SVD), deep retinal capillary layer vascular density (DVD), and choroidal blood capillary layer blood flow density (CFD). Multifocal visual electrophysiology equipment provided latency and amplitude of N1 and P1 waves. Differences and changes among the four Grade of fundus tessellation grading were compared, and ROC curve analysis was performed to identify the optimal choroidal thickness indicators for predicting the grading of fundus tessellation.

Results: SFCT tends to decrease as the grade of fundus tessellation increases. and the amplitudes of N1 and P1 waves in multifocal electroretinography reduce, with an elongation in their latency periods. Correlation analysis showed that SFCT positively correlated with N1 and P1 amplitudes ($r=0.270$, 0.246; $P<0.05$) and negatively correlated with their latency periods ($r=-0.219$, -0.248; $P<0.05$). The ROC curve results indicated the cutoff values for SFCT were 192.75μm between Grade 1 and 2, 162μm between Grade 2 and 3, and 130.75μm between Grade 3 and 4.

Conclusion: Assessment in fundus tessellation using MfERG and OCTA contributes to objective grading of fundus tessellation and further help to clinical prediction and treatment.

Translational Relevance: Assessment in fundus tessellation morphologically and functionally using MfERG and OCTA contributes to classification and clinical prediction of fundus tessellation.

Keywords: fundus tessellation, multifocal electrophysiology, optical coherence tomography angiography, myopia, classification

INTRODUCTION

Myopia is a common refractive error, with its global prevalence progressively climbing and expected to reach 50% by 2050[1]. Myopia-related pathological changes are becoming one of the primary causes of visual impairment and blindness[2]. Therefore, the early detection of myopic fundus progression and effectively reducing the incidence of high myopia has become a significant public health concern worldwide. This is particularly concerning, as high myopia is linked to an elevated risk of vision impairment and various sight-threatening complications, including glaucoma, cataracts, retinal detachment, and myopic maculopathy[35]. Cover, as the degree of myopia increases, a series of pathological changes can occur in the fundus, including Fundus Tessellation (FT), peripapillary atrophic crescents, thinning of the retinal pigment epithelium, Fuchs' spots, and choroidal-retinal atrophy[3]. The formation mechanism of a FT is complex. Some researchers [13] suggest that it is caused by the loss of retinal pigment epithelial cells, increased permeability of the retinal pigment epithelium, reduced choroidal capillary perfusion, and thinning of the choroid. Choroidal thinning progresses most rapidly in the macular-papillary region due to the proximity of the fundus mosaic to the fovea[39-40].

Fundus tessellation is a specific subtype of myopic maculopathy, marked by the presence of prominent choroidal vessels in the fundus. This condition may advance to more severe forms of myopic maculopathy, leading to serious complications such as choroidal neovascularization and macular atrophy, which can result in significant visual impairment or even disability. Early detection and appropriate management are crucial to preventing progression and reducing the impact on visual health[36]. Among

these, fundus tessellation changes are often the earliest natural course of myopic fundus diseases and are an important clinical marker of retinal disease progression[4].

Fundus tessellation is characterized by clearly visible large choroidal vessels at the posterior pole of the eye, appearing as leopard-spot-like patterns due to the structural arrangement of choroidal vessels and pigment gaps. The META-PM classification system categorizes myopic macular changes into four types, with fundus tessellation changes classified as Type I[5]. FT is the most common form of myopic fundus change, particularly prevalent in China, a country with high incidence of myopia, where more than half of highly myopic adolescents exhibit fundus tessellation changes[6].Studies have shown that in patients with a refractive error less than -10.00D, the probability of developing fundus tessellation is 85.7%[7].

Currently, several methods exist for grading fundus tessellation. Yan et al[8]. classified the severity of fundus tessellation based on the visibility of large choroidal vessels in 45° fundus photographs of the macula and optic disc area, dividing it into four grades: from Grade 0 (no fundus tessellation changes) to Grade 3 (severe fundus tessellation changes). Subsequent longitudinal studies have refined this classification into eight more detailed grades. Some studies have used the ETDRS(Early Treatment Diabetic Retinopathy Study) grid on fundus photographs to grade the relative position between fundus tessellation and the macular fovea[9], which defined grade 0 as invisible choroidal great vessels, grade 1 as posterior extremely visible choroidal great vessels but not involving ETDRS grid, grade 2 as FT visible in the outer ring of ETDRS grid but not involving the middle ring, and grade 3 as FT visible in the middle ring of ETDRS grid but not involving the inner macular fovea. Grade 4 shows visible large choroidal vessels within the inner circle of the ETDRS grid at the fovea, suggesting that the assessment of the

relative position of fundus tessellation to the macular fovea may be an ideal standard for evaluating the severity of fundus tessellation changes.

The formation mechanism of fundus tessellation is not entirely clear, but it is thought to be caused by the loss of retinal pigment epithelial cells, increased translucency of the retinal pigment epithelium, decreased perfusion of choroidal capillaries, and thinning of the choroid[10]. Currently, the grading of fundus tessellation lacks objective quantifiable indicators, and the corresponding changes in morphological and functional features of the retina and choroid associated with fundus tessellation changes are not well defined. Clearly defining the grading of high myopia with fundus tessellation, exploring the changes in morphology and function of the retina and choroid at different grades, and further quantifying these changes can provide new approaches for the early detection and control of pathological changes in myopic fundus. Recent advancements in imaging technologies have enhanced the observation of pathological changes in myopia. Multifocal electroretinography (MfERG) detects local electrophysiological activity in the retina. Studies show that the first-order response of MFERG decreases with increasing myopia severity, indicating functional impairment of photoreceptor cells[37]. Optical coherence tomography (OCT) allows in vivo imaging of retinal and choroidal cross-sections, facilitating the study of fundus tessellation in relation to retinal, choroidal, and scleral thickness[38]. Optical coherence tomography angiography (OCTA) extends OCT, enabling quantitative analysis of blood flow density, area of perfused regions, and the avascular zone in the fovea.

Therefore, this study aims to assess fundus tessellation morphologically and functionally using MfERG and OCTA to explore the differences in retinal and choroidal morphology and function among patients with different grades of fundus tessellation changes. This will guide more objective grading of

fundus tessellation and further use these changes as markers to identify morphology, function, degree of myopia, and risk of progression.

MATERIALS AND METHODS

Patients

Patients with high myopia (SE ≤ -6D) and accompanying fundus tessellation were selected from those who visited the Ningbo City Eye Hospital from March 2021 to February 2023. This study included 52 patients with fundus tessellation changes, totaling 87 eyes, consisting of 30 male eyes and 57 female eyes. The ages ranged from 18 to 50 years, with an average age of 31.45 ± 8.63 years. The spherical equivalent ranged from -6D to -15D, with an average spherical equivalent of -8.48 ± 1.85D. The axial lengths ranged from 25.09 mm to 33.24 mm, with an average axial length of 27.19 ± 1.53 mm. The trial adhered to the Declaration of Helsinki and was approved by the ethics committee of Ningbo City Eye Hospital (No. 2023022), with informed consent obtained from all participants.

Inclusion Criteria: Patients with high myopia (SE ≤ -6D) aged between 18 and 50 years; Clear refractive media with good fixation ability, able to provide high-quality retinal photographs; No history of eye surgery or trauma except for myopia correction surgeries; No other ocular diseases that could cause changes in the fundus appearance, such as primary open-angle glaucoma or choroidal vascular disorders; No severe systemic diseases such as heart disease, hypertension, or diabetes; Complete and reliable MfERG and OCTA examination data.

Exclusion Criteria: Concurrent other eye diseases, such as primary open-angle glaucoma, age-related macular degeneration, choroidal vascular changes, or other macular diseases; Poor vision and fixation

ability, unable to cooperate with examinations; Cloudy refractive media, such as severe cataract without fixation ability, unable to complete all examinations; Severe systemic diseases, such as uncontrolled diabetes, hypertension, or cardiopulmonary dysfunction.

The ETDRS grid is typically composed of multiple concentric circles and sector regions, facilitating systematic recording and assessment of lesions during retinal examinations. The ETDRS grid uses the center of the fovea as the origin, dividing the macular area into three concentric circular regions: the foveal area zone (SF) with a diameter of 1 mm, the inner ring (I) with a diameter of 3 mm, and the outer ring (O) with a diameter of 6 mm. Both the inner and outer ring zones are further subdivided into four sectors: superior (S), temporal (T), inferior (I), and nasal (N), which are sequentially labeled as IS, IT, II, IN, OS, OT, OI, and ON.

Lesion Classification Criteria: Lesions were classified using the ETDRS grid on fundus photographs (Figure 1): Group 1 (21 eyes): Grade 1 fundus tessellation, defined as visible large choroidal vessels at the posterior pole without involving the ETDRS grid. Group 2 (20 eyes): Grade 2 fundus tessellation, defined as visible large choroidal vessels at the outer ring of the ETDRS grid but not involving the inner ring. Group 3 (21 eyes): Grade 3 fundus tessellation, defined as visible large choroidal vessels within the inner ring of the ETDRS grid but not involving the macular fovea. Group 4 (24 eyes): Grade 4 fundus tessellation, defined as visible large choroidal vessels within the innermost circle of the ETDRS grid at the macular fovea.

Image Acquisition and Analysis

All patients underwent a preliminary consultation including a detailed history of baseline diseases followed by routine ophthalmological examinations. These examinations included uncorrected and corrected visual acuity tests, slit-lamp microscopy examination of the anterior segment, non-contact tonometry for intraocular pressure (IOP) measurement, biometry with the IOL-Master to measure axial lengths (AL, IOL Master, Carl Zeiss, Tubingen, Germany), fundus photography (FP, KOWA nonmyd7, Japan). Fundus photographs of the macular and optic disc areas at 45° were taken with adequate exposure and clear focus. Images with indiscernible fundus tessellation were excluded from the study.

OCTA Examination

All subjects were examined using the spectral domain system, Spectralis OCTA (Heidelberg Engineering, Heidelberg, Germany). In Enhanced Depth Imaging (EDI) mode, the scanning lens focused on the center of the pupil and gradually moved forward, ensuring the image was clear and centered with uniform signal intensity and brightness. The study used a 3mm × 3mm scanning mode centered on the macular fovea, with each location spaced 12.2μm apart and each location undergoing four repeated B-scans. The total time for scanning a single blood flow image was 2-3 seconds. This device's unique eye-tracking technology was used to save only those images that met quality standards. The clearest EDI-OCT images of the choroid were used to measure SFCT, defined as the distance from the outer edge of the highly reflective line of the retinal pigment epithelium (RPE) to the inner layer of the sclera. MT and RPE thickness were also measured (Figure 2A). Images of the SVD, DVD, and CFD were obtained through automatic layering (Figure 2B-D). The boundaries for SCP were set from 3μm below the inner limiting membrane to 15μm below the inner plexiform layer, and for the DCP from 15μm to 70μm below the

inner plexiform layer. The choroidal capillary layer was defined from 30μm to 60μm below the reference plane of the RPE. ImageJ software was used to calculate the vascular density of these layers, recording the MT, RPE, and SFCT, as well as the vascular density of the SVD, DVD, and CFD.

MfERG Examination

Multifocal electroretinography (MfERG) measures localized retinal electrical responses under photopic conditions, providing a topographic map of retinal function. The technique uses a hexagonal 61-element stimulation array arranged concentrically, which alternates light and dark in a pseudorandom sequence to stimulate specific retinal regions. The electrical responses are recorded from the central retina (ring 1) to the peripheral retina (ring 5) using electrodes(Figure 3B). A typical MfERG waveform consists of an initial negative peak (N1) and a subsequent positive peak (P1). N1 amplitude is measured from the baseline to the trough, and P1 amplitude is measured from the trough of N1 to the peak of P1(Figure 3A)[40]. Latency is calculated as the time from the stimulus onset to each peak. All patients underwent MfERG examination (Metrovision, France) of the affected eye according to the inclusion criteria. The frame rate of the stimulator was 60 Hz, covering a visual field of approximately 30° . The stimulus pattern consisted of 61 hexagons of equal size arranged concentrically. The bandpass was set between 5 and 100 Hz, with a response sampling rate of about 1000 Hz, translating to an interval of 0.98 ms between responses. Subjects were adapted to ordinary room light for 15 minutes before the test, and it was recommended to avoid fundus examinations or fundus photography within 12 hours prior to the test. Pupils were dilated with compound tropicamide, and after topical corneal anesthesia, a Jet contact lens recording electrode was placed. A silver disc reference electrode was positioned on the skin at the lateral

canthus of the same side, and a ground electrode was placed on the forehead skin. Subjects were instructed to concentrate on fixating on a red cross in the center of the screen and to avoid blinking. Ultimately, we were able to obtain numerical values for each waveform array (see Figures 3C,D).

Statistical Analysis

Data analysis was performed using SPSS statistical software version 26.0. All quantitative data were subjected to the Kolmogorov-Smirnov test for normality. For data following a normal distribution, the mean and standard deviation (x±s) were used for representation. Comparisons between groups were conducted using one-way ANOVA, with post-hoc pairwise comparisons performed using the LSD test. For data not following a normal distribution, the median and interquartile range were used, and comparisons between groups were made using the Kruskal-Wallis H test, with pairwise comparisons adjusted using the Bonferroni method. Categorical data were represented by proportions, and comparisons between groups were made using the Chi-square test. Multiple linear regression analysis was used to study the influencing factors among the four groups. Pearson correlation analysis was employed to examine the relationships between SFCT and the amplitude and latency of the N1 and P1 waves, as well as the correlation between three types of blood flow density (SVD, DVD, CFD) and the amplitude and latency of the N1 and P1 waves. Finally, ROC curve analysis was utilized to assess the predictive value of SFCT across different grades of FT. A p-value of less than 0.05 was considered statistically significant.

RESULTS

Patient selection

This study included 52 patients with fundus tessellation changes, totaling 87 eyes, with 30 male e yes and 57 female eyes. There were 21 eyes in Grade 1, 20 eyes in Grade 2, 22 eyes in Grade 3, and 24 eyes in Grade 4. The age range was 15 to 50 years, with an average age of 31.45 ± 8.63 years. The SE ranged from -6.0D to -15D, with an average SE of -8.48 ± 1.85D. The AL ranged from 25.09mm to 33.24mm, with an average of 27.19 ± 1.53mm.

Statistically significant differences were observed in the SE and AL across different grades of FT ($P<0.05$). Pairwise comparisons between groups revealed that the SE in Grade 2, 3, and 4 w as significantly lower than in Grade 1 ($P<0.05$). The axial length in Grade 4 was longer than in Grade 1 and 2, with significant differences ($P<0.05$). There were no statistically significant differe nces in age, gender, or intraocular pressure across the groups ($P>0.05$) (Table 1).

Comparison of the thickness of anatomical layer, vascular density and MfERG of fundus tessellation.

Statistically significant differences were observed in the SFCT across different grades of fundus tessellation ($P<0.05$). Pairwise comparisons between groups showed that SFCT was thinner in Grade 2, 3, and 4 compared to Grade 1, with all differences being statistically significant ($P<0.05$). Compared to Grade 4, SFCT was thicker in Grade 2 and 3, with these differences also being statistically significant ($P<0.05$). No significant differences were found in MT and RPE across the groups ($P>0.05$) (Table 2).

Significant differences in the SVD were observed among different grades of FT ($P<0.05$). Pairwise comparisons indicated that SVD was higher in Grade 1, 2, and 4 compared to Grade 3, with all differences being statistically significant ($P<0.05$). No significant differences were found in the DVD and CFD across the groups ($P>0.05$) (Table 2).

Statistically significant differences were observed in the amplitudes and latencies of total N1 and P1 waves of MfERG across different grades of FT ($P<0.05$). Pairwise comparisons showed that the amplitudes of N1 waves were lower in Grade 2, 3, and 4 compared to Grade 1, with all differences being statistically significant ($P<0.05$). The amplitudes of N1 waves in Grade 3 and 4 were also lower than in Grade 2, with significant differences ($P<0.05$). Similarly, the amplitudes of P1 waves in Grade 3 and 4 were lower than in Grade 1, with significant differences ($P<0.05$). Compared to Grade 4, the amplitudes of P1 waves were higher in Grade 2 and 3, with statistically significant differences ($P<0.05$). The latency periods of N1 waves were longer in Grade 3 and 4 compared to Grade 1, with all differences being statistically significant ($P<0.05$). The latency period of N1 waves in Grade 4 was longer than in Grade 2, with a significant difference ($P<0.05$). The latency periods of P1 waves were also longer in Grade 3 and 4 compared to Grade 1, with significant differences ($P<0.05$); the latency period of P1 waves in Grade 4 was longer than in Grade 2, also showing a significant difference ($P<0.05$). Overall, as the grade of FT increased, SFCT decreases, and the amplitudes of N1 and P1 waves decreased, while their latency periods correspondingly increased (Table 2). These trends are important because they demonstrate a clear correlation between structural changes (SFCT thinning) and functional deficits (MfERG amplitudes). This underscores the value of combining anatomical and functional assessments for evaluating and predicting disease progression in patients with myopic fundus tessellation. Understanding these relationships could guide earlier interventions to prevent vision loss.

Comparison of MfERG N1 and P1 Wave Amplitudes and Latencies Across Different Rings in Different Grades of Fundus tessellation (FT)

As the grade increase, the amplitudes of N1 and P1 waves in rings 1-5 of MfERG progressively decrease across different grades of FT, with significant decreases in amplitude from ring to ring within each group ($P<0.05$) (Fig 4, Tables S1, S2).

Significant differences were found in the latency periods of N1 waves in rings 1, 3, and 4 across different grades of FT ($P<0.05$). Pairwise comparisons showed that the latency period of ring 1 in Grade 4 was longer than in the other three grades. Compared to Grade 1, the latency periods of ring 4 increased in Grade 2, 3, and 4. The latency period of ring 5 in Grade 4 was longer than in Grade 1. All these differences were statistically significant ($P<0.05$) (Fig 4, Table S3).

Significant differences were also observed in the latency periods of P1 waves in rings 1, 2, and 4 across different grades of FT ($P<0.05$). Pairwise comparisons indicated that the latency periods of ring 1 in Grade 3 and 4 were longer than in Grade 1, with Grade 4's ring 1 latency period being longer than in Grade 2. The latency period of ring 2 in Grade 3 was longer than in Grade 1 and 2, and the latency period of ring 2 in Grade 4 was longer than in the other three grades. The latency period of ring 4 in all groups was shorter than in Grade 1. All these differences were statistically significant ($P<0.05$) (Fig 4, Table S4).

Logistic Regression

Logistic regression analysis demonstrating the relationship between subfoveal choroidal thickness (SFCT), N1 wave amplitude, and P1 wave latency with the severity of fundus tessellation. The analysis shows that as the grade of fundus tessellation increases, SFCT decreases significantly ($\beta = -0.034$, $P = 0.001$), reflecting choroidal thinning. N1 wave amplitudes decrease ($\beta = -0.407$, $P = 0.001$), indicating reduced retinal function, and P1 wave latencies increase ($\beta = 0.465$, $P = 0.007$), suggesting delayed visual

information transmission. These findings emphasize the importance of SFCT as a structural biomarker and MfERG parameters as functional biomarkers for assessing fundus tessellation progression.

(Table 3).

Correlation Analysis between Choroidal Thickness and N1/P1 Wave Amplitudes and Latencies in Patients with Fundus tessellation

Pearson correlation analysis of subfoveal choroidal thickness (SFCT) with N1 and P1 amplitudes and latencies. A positive correlation was observed between SFCT and N1/P1 amplitudes ($r = 0.270$ and $r = 0.246$, respectively, $P < 0.05$), indicating that thicker choroids are associated with better retinal function. Conversely, a negative correlation was found between SFCT and N1/P1 latencies ($r = -0.219$ and $r = -0.248$, respectively, $P < 0.05$), suggesting that choroidal thinning delays visual information transmission. These findings underscore the interplay between structural choroidal changes and functional retinal decline, highlighting SFCT as a critical biomarker for myopic progression(Figure5,Table4).

Correlation Analysis Between Blood Flow Density and N1/P1 Wave Amplitudes and Latencies in Patients with Fundus tessellation

Pearson correlation analysis of superficial retinal capillary layer vascular density (SVD), deep retinal capillary layer vascular density (DVD), and choroidal blood flow density (CFD) with N1 and P1 amplitudes and latencies. No statistically significant correlations were observed between vascular densities (SVD, DVD, CFD) and MfERG metrics ($P > 0.05$), indicating that retinal and choroidal blood flow density may not directly affect retinal electrical function in fundus tessellation. This finding suggests that microvascular changes may operate independently of electrophysiological activity in the early stages of myopic changes. (Table 5).

ROC Curve Analysis of Choroidal Thickness in Fundus tessellation

Figure 6 shows the ROC curves for SFCT (subfoveal choroidal thickness) across different grades of fundus tessellation (FT). The cutoff values and corresponding performance metrics are as follows:Grade 1 vs. Grade 2: Cutoff at 192.75 μm, sensitivity 76.2%, specificity 90.0%, AUC 0.820, indicating excellent predictive performance for distinguishing between these two grades(Figure 6A).Grade 2 vs. Grade 3: Cutoff at 162 μm, sensitivity 70.0%, specificity 68.2%, AUC 0.695, suggesting moderate predictive performance(Figure 6B).Grade 3 vs. Grade 4: Cutoff at 130.75 μm, sensitivity 81.8%, specificity 66.7%, AUC 0.741(Figure 6C).These results indicate that SFCT is a useful biomarker for grading FT severity, particularly effective in distinguishing earlier grades. However, the varying AUC values suggest limitations in differentiating more advanced stages.

Although the AUC for this cutoff value is excellent, this study did not conduct validation trials to verify the effectiveness of this cutoff in practice. Therefore, our cutoff SFCT values should be considered as a complementary method alongside fundus photography. The results show that the cutoff value between Grade 1 and Grade 2 FT is 192.75μm, between Grade 2 and Grade 3 is 162μm, and between Grade 3 and Grade 4 is 130.75μm, as shown in Table 6. This study did not include eyes without FT changes, i.e., normal eyes were not assessed for SFCT values. Thus, the results indicate: SFCT > 192.75μm for Grade 1 FT or eyes without any pathologic myopic fundus changes; SFCT between 162μm and 192.75μm for Grade 2 FT; SFCT between 130.75μm and 162μm for Grade 3 FT; and SFCT < 130.75μm for Grade 4 FT or even more severe myopic macular changes. These results underscore the value of SFCT as an objective biomarker for differentiating between grades of fundus tessellation, thereby enhancing early detection and monitoring of disease progression.

DISCUSSION

Changes in fundus tessellation, representing early lesions in pathologic myopia, are crucial for clinical intervention and research. In 2015, an international expert group led by Ohno-Matsui categorized fundus tessellation as category 1, the earliest stage of pathologic myopic maculopathy.[5] This study utilized the ETDRS grid to grade the relative positions of myopic fundus tessellation changes and the macular fovea (Figure 1), proposing that assessing these positions could be an ideal standard for evaluating the severity of myopic fundus tessellation changes. Terasaki et al[11]. have shown that the distribution of fundus tessellation is significant for explaining and predicting myopic changes. The presence of fundus tessellation may indicate a high risk of myopic fundus lesions, with approximately 19-22% and 20-30% of eyes with fundus tessellation changes progressing to pathologic myopia[12,13]. All these findings suggest that the presence of fundus tessellation might indicate further progression of myopic fundus changes, serving as a foundation for pathologic myopic fundus lesions. In some myopic patients, fundus tessellation changes may persist for an extended period, while others may develop more severe macular lesions, potentially leading to irreversible vision loss.

Previous literature reports that increasing diopters is a risk factor for fundus tessellation changes[12]. Foo et al[14]. found that in adults with myopia but no pathologic fundus changes, fundus tessellation, age, axial length, and refraction are good predictors of pathologic myopia. These findings are consistent with our study results, which show statistically significant differences in SE and AL among different FT grades ($P<0.05$), with the SE of Grade 1 FT being the highest and the axial length of Grade 4 being longer than Grade 1 and 2. Zhao et al. [15] found that AL growth is closely related to choroidal thinning, primarily leading to a decrease in the thickness of large (Haller's layer) and medium (Sattler's layer) vascular layers.

Thus, the proportion of small vessels in the total choroidal thickness increases with AL growth, deepening the degree of fundus tessellation.

Due to the atrophy of the RPE and choroidal capillary layer and pigment loss in choroidal tissue, fundus tessellation is most evident in the posterior pole. This study analyzed the relationship between different grades of high myopia fundus tessellation changes and changes in MT, RPE, and SFCT, finding a clear correlation between FT and SFCT; higher FT grades correspond to thinner SFCT. Some researchers believe that early changes in fundus tessellation are related to thinner choroid[16,17]. Progressive choroidal thinning has been identified as a core factor in the transition from no change to FT change. Yan et al.[13] also indicated that choroidal thinning is significantly correlated with the degree of FT, making fundus tessellation a clinical indicator of choroidal thinning. The grading of FT in this study gradually extends from the peripheral fundus to the macular fovea, with choroidal thinning not clearly evident in Grade 1 FT. As myopia progresses with axial length growth, mechanical stretching of the choroid can explain the high incidence of fundus tessellation[18]. Numerous studies confirm that as the degree of myopia deepens, choroidal thinning becomes more pronounced[19,20]. The retinal thickness shows a progressive thinning trend with increasing severity of fundus tessellation[21]. Although this study did not design measurements for peripheral retinal thickness, measurements were taken for the thickness of the macular fovea and RPE layer, finding no significant impact of fundus tessellation changes on MT or RPE. We speculate that this limitation is due to measurements only being taken at the foveal center and not the retinal periphery.

While numerous studies have investigated retinal blood flow in myopia, reports on changes in retinal vascular density at different FT grades are scarce. Current research indicates that myopia complications are closely related to morphological changes in retinal vessels, but studies on microcirculation in myopic fundus

remain controversial[22]. Therefore, this study analyzed and compared retinal and choroidal blood flow density in fundus tessellation changes. Our results show that the superficial retinal capillary layer vascular density in the macular region decreases with increasing fundus tessellation grade (Table 2), consistent with previous study[23]. Multiple studies have demonstrated that before significant pathologic myopic fundus changes occur, macular vascular density decreases with deepening myopia[24,25]. Some studies even suggest that from mild to high myopia, the vascular density of both the superficial and deep retinal layers gradually decreases[26]. Yang et al[27]. also indicated that varying degrees of myopia do not affect the vascular density of the macular region in young, healthy adults. Research on macular retinal layered blood flow and choroidal blood flow is relatively scarce, with inconsistent results in existing literature. We speculate that this may be related to the ease of neovascularization and macular bleeding in later stages of high myopia, which still requires further exploration. Our study observed a declining trend in superficial retinal capillary plexus vascular density in the macula region up to Grade 3 FT, with an increase in Grade 4 (Table 2). After excluding other pathologic high myopia fundus changes, can we consider that severe FT eyes exhibit a compensatory increase in SVD? Choroidal capillary layer blood flow density also shows no significant change.

Furthermore, this study indicates that aside from SVD, differences in DVD and CFD in relation to the severity of fundus tessellation changes are not statistically significant (all $P>0.05$) (Table 2), possibly related to the selected measurement area. This study only chose a 3mm x 3mm range within the macula and did not analyze and compare the entire macular retina and choroid. Local blood flow results cannot fully represent overall retinal blood flow changes unrelated to FT. On the other hand, this may be due to the deep retinal circulation in the macula being nourished by the choroidal circulation.

MfERG can simultaneously test functional changes in multiple areas of the macular retina, valuable for assessing retinal function. To confirm whether the macular central area exhibits functional abnormalities when early FT changes have not yet appeared, this study first analyzed changes in the amplitude density and latency of MfERG in different grades of myopic fundus tessellation. We found that as the degree of fundus tessellation changes deepened, the amplitudes of MfERG's N1 and P1 waves decreased, while their latency periods lengthened. This is consistent with the conclusions of numerous studies[28-30]. Our results also show that the amplitudes of MfERG's N1 and P1 waves are highest in ring 1 in all grades, gradually decreasing from the central to peripheral rings, with the most significant differences in ring 1 (Table 2). Thus, as the degree of FT increases, the amplitudes of N1 and P1 waves continuously decline, while their latency periods correspondingly lengthen.

However, research on MfERG changes in myopic fundus tessellation is limited. Hamzawy et al[31]. believe that the amplitude of various waves in MfERG decreases with increasing axial length in myopic eyes without pathologic fundus changes. Some scholars have explored MfERG, finding that as the spherical equivalent increases, its amplitude decreases, and latency lengthens, with myopia initially manifesting as a loss of cone function, possibly occurring even without significant changes in fundus appearance[31]. Based on this, we speculate that when Grade 1 fundus tessellation changes occur, the affected eye has likely already undergone visual function changes. However, other researchers believe that the first-order MfERG response's P1 wave may originate from retinal bipolar cells[32]. The decline in average amplitude density of the P1 wave suggests bipolar cell dysfunction, while changes in latency indicate alterations in neural information transmission in the visual pathway.

Visual electrophysiological changes in young people with high myopia may precede fundus and OCT changes, indicating that morphological and functional changes in the retinal retina are closely related, consistent with the results of this study. Our study analyzed the correlation between SFCT and the amplitudes and latencies of N1 and P1 waves, finding that in myopic fundus tessellation changes, both N1 and P1 amplitudes decrease with thinning SFCT, while N1 and P1 latencies lengthen (Figure 4).

MfERG provides information on macular function, while OCTA shows structural changes in macular blood flow. Currently, there are few joint reports on the morphology and function of fundus tessellation. Our study combined OCTA and MfERG for a comprehensive analysis of the morphology and function of retinal cells and blood flow in myopic fundus tessellation photos, providing new insights for research on pathologic myopia. Palmersky-Wolf has shown that morphological tests like OCTA cannot replace retinal functional tests like MfERG[34]. In many cases, retinal function damage exists before significant morphological changes in the retina. Therefore, discussing changes in pathologic myopia should not only focus on its morphological changes but also its functional transitions. MfERG is a very valuable testing method, especially when retinal structural changes are not obvious, but functional changes are present. OCTA is very sensitive to changes in the macular structure and can reveal overlooked MfERG changes. Both can complement each other, providing a comprehensive assessment of retinal function and morphology.

This study still has certain limitations. First, the determination of FT Grade requires subjective judgment by a human, so to avoid subjective errors, it needs to be reviewed by experienced physicians to ensure the accuracy of the results as much as possible. Secondly, multiple measurements are needed to reduce measurement errors. In the future, it is necessary to expand the sample size as much as possible to

provide more complete data support for myopic fundus lesions. Furthermore, since the included patients were sourced from a single hospital, there may be a certain bias in the sample. Future studies could expand the patient inclusion criteria and increase the sample size to enhance the generalizability of the results.

Conclusion

The degree of myopic fundus tessellation changes is positively correlated with axial length and negatively correlated with spherical equivalent. As the degree of myopic fundus tessellation deepens, the thickness under the central fovea choroid thins, and the amplitudes of N1 and P1 waves decrease, while their latency periods lengthen, and as SFCT thins, the amplitudes and latency periods of N1 and P1 waves also change. FT Grade 1 or before pathologic myopic fundus changes occur, SFCT > 192.75μm; FT Grade 2 SFCT is between 162μm and 192.75μm; FT Grade 3 SFCT is between 130.75μm and 162μm; FT Grade 4 or when more severe pathologic myopic fundus changes occur, SFCT < 130.75μm.

Through appropriate examinations of the fundus tessellation changes, we analyze the structural, functional, and blood flow characteristics of the mottled fundus lesions. A comprehensive assessment of these examinations allows for the early detection and quantification of lesions, thereby enhancing the detection rate of fundus changes in high myopia. This has significant implications for guiding clinical treatment. Furthermore, these indicators can be utilized to monitor treatment efficacy and track disease progression, laying a foundation for the early prevention and management of pathologic myopia and visual health.

Abbreviations

Multifocal visual electrophysiology: MfERG, Optical coherence tomography angiography: OCTA, High Myopia: HM, Macular foveal thickness: MT, Retinal pigment epithelium: RPE, Subfoveal choroidal thickness: SFCT, Superficial retinal capillary layer vascular density: SVD, Deep retinal capillary layer vascular density: DVD, Choroidal blood capillary layer blood flow density: CFD, Spherical equivalent: SE, Axial length: AL, Fundus tessellation: FT, Early Treatment Diabetic Retinopathy Study: ETDRS, Retinal pigment epithelium: RPE, Fundus tessellation: FT, IOP: Intraocular pressure; bcva: Best corrected visual acuity; CT: Choroidal thickness, Receiver-operating characteristic curve: ROC.

Competing interests

The authors report no conflicts of interest in this work.

References

1. Holden BA, Fricke TR, Wilson DA, et al. Global prevalence of myopia and high myopia and temporal trends from 2000 through 2050. *Ophthalmology*. 2016;123(5):1036-1042. doi:10.1016/j.ophtha.2016.01.006
2. Jonas JB, Jonas RA, Xu J, Wang YX. Prevalence and cause of loss of visual acuity and visual field in highly myopic eyes: The Beijing Eye Study. *Ophthalmology*. 2024;131(1):58-65. doi:10.1016/j.ophtha.2023.08.026
3. Hopf S, Pfeiffer N. Epidemiologie der Myopie. *Ophthalmologe*. 2017;114(1):20-23. doi:10.1007/s00347-016-0361-2
4. Jonas JB, Gründler A. Optic disc morphology in "age-related atrophic glaucoma". Graefes Arch Clin Exp Ophthalmol. 1996;234(12):744-749. doi:10.1007/BF00189355
5. Ohno-Matsui K, Kawasaki R, Jonas JB, et al. International photographic classification and grading system for myopic maculopathy. *Am J Ophthalmol*. 2015;159(5):877-83.e7. doi:10.1016/j.ajo.2015.01.022
6. Wong YL, Ding Y, Sabanayagam C, et al. Longitudinal changes in disc and retinal lesions among Hhighly myopic adolescents in Singapore over a 10-Year period. *Eye Contact Lens*. 2018;44(5):286-291. doi:10.1097/ICL.0000000000000466
7. Koh VT, Nah GK, Chang L, et al. Pathologic changes in highly myopic eyes of young males in Singapore. *Ann Acad Med Singap*. 2013;42(5):216-224
8. Yan YN, Wang YX, Xu L, Xu J, Wei WB, Jonas JB. Fundus tessellation: Prevalence and associated factors: The

Beijing Eye Study 2011. *Ophthalmology*. 2015;122(9):1873-1880. doi:10.1016/j.ophtha.2015.05.031

9. Lyu H, Chen Q, Hu G, et al. Characteristics of fundal changes in fundus tessellation in young adults. *Front Med (Lausanne)*. 2021;8:616249. doi:10.3389/fmed.2021.616249

10. Switzer DW Jr, Mendonça LS, Saito M, Zweifel SA, Spaide RF. Segregation of ophthalmoscopic characteristics according to choroidal thickness in patients with early age-related macular degeneration. *Retina*. 2012;32(7):1265-1271. doi:10.1097/IAE.0b013e31824453ac

11. Terasaki H, Yamashita T, Yoshihara N, et al. Location of tessellations in ocular fundus and their associations with optic disc tilt, optic disc area, and axial length in young healthy Eyes. *PLoS One*. 2016;11(6):e0156842. doi:10.1371/journal.pone.0156842

12. Yan YN, Wang YX, Yang Y, et al. Ten-year progression of myopic maculopathy: The Beijing Eye Study 2001-2011. *Ophthalmology*. 2018;125(8):1253-1263. doi:10.1016/j.ophtha.2018.01.035

13. Fang Y, Yokoi T, Nagaoka N, et al. Progression of Myopic Maculopathy during 18-Year Follow-up. *Ophthalmology*. 2018;125(6):863-877. doi:10.1016/j.ophtha.2017.12.005

14. Foo LL, Xu L, Sabanayagam C, et al. Predictors of myopic macular degeneration in a 12-year longitudinal study of Singapore adults with myopia. *Br J Ophthalmol*. 2023;107(9):1363-1368. doi:10.1136/bjophthalmol-2021-321046

15. Zhao J, Wang YX, Zhang Q, Wei WB, Xu L, Jonas JB. Macular choroidal small-vessel layer, Sattler's layer and Haller's layer thicknesses: The Beijing Eye Study. *Sci Rep*. 2018;8(1):4411. doi:10.1038/s41598-018-22745-4

16. Cheng T, Deng J, Xu X, et al. Prevalence of fundus tessellation and its associated factors in Chinese children and adolescents with high myopia. *Acta Ophthalmol*. 2021;99(8):e1524-e1533. doi:10.1111/aos.14826

17. Fang Y, Du R, Nagaoka N, et al. OCT-Based diagnostic criteria for different stages of myopic maculopathy. *Ophthalmology*. 2019;126(7):1018-1032. doi:10.1016/j.ophtha.2019.01.012

18. Postolache L, De Jong C, Casimir G. Illustration of tessellation in Down syndrome. *Ophthalmic Genet*. 2020;41(2):135-145. doi:10.1080/13816810.2020.1744021

19. El-Shazly AA, Farweez YA, ElSebaay ME, El-Zawahry WMA. Correlation between choroidal thickness and degree of myopia assessed with enhanced depth imaging optical coherence tomography. *Eur J Ophthalmol*. 2017;27(5):577-584. doi:10.5301/ejo.5000936

20. Jagadeesh D, Philip K, Naduvilath TJ, et al. Fundus tessellation appearance and its association with myopic refractive error. *Clin Exp Optom*. 2019;102(4):378-384. doi:10.1111/cxo.12822

21. Pang Y, Goodfellow GW, Allison C, Block S, Frantz KA. A prospective study of macular thickness in amblyopic children with unilateral high myopia. *Invest Ophthalmol Vis Sci*. 2011;52(5):2444-2449. doi:10.1167/iovs.10-5550

22. Kim YM, Yoon JU, Koh HJ. The analysis of lacquer crack in the assessment of myopic choroidal neovascularization. *Eye (Lond)*. 2011;25(7):937-946. doi:10.1038/eye.2011.94

23. Li M, Yang Y, Jiang H, et al. Retinal microvascular network and microcirculation aAssessments in high myopia. *Am J Ophthalmol*. 2017;174:56-67. doi:10.1016/j.ajo.2016.10.018

24. Yang Y, Wang J, Jiang H, et al. Retinal microvasculature alteration in high myopia. *Invest Ophthalmol Vis Sci*. 2016;57(14):6020-6030. doi:10.1167/iovs.16-19542

25. Al-Sheikh M, Phasukkijwatana N, Dolz-Marco R, et al. Quantitative OCT angiography of the retinal microvasculature and the choriocapillaris in myopic eyes. *Invest Ophthalmol Vis Sci*. 2017;58(4):2063-2069. doi:10.1167/iovs.16-21289

26. Liu M, Wang P, Hu X, Zhu C, Yuan Y, Ke B. Myopia-related stepwise and quadrant retinal microvascular alteration and its correlation with axial length. *Eye (Lond)*. 2021;35(8):2196-2205. doi:10.1038/s41433-020-01225-y

27. Yang S, Zhou M, Lu B, et al. Quantification of macular vascular density using optical coherence tomography angiography and its relationship with retinal thickness in myopic eyes of young adults. *J Ophthalmol*. 2017;2017:1397179. doi:10.1155/2017/1397179

28. Sachidanandam R, Ravi P, Sen P. Effect of axial length on full-field and multifocal electroretinograms. *Clin Exp Optom*. 2017;100(6):668-675. doi:10.1111/cxo.12529

29. Ismael ZF, El-Shazly AAE, Farweez YA, Osman MMM. Relationship between functional and structural retinal changes in myopic eyes. *Clin Exp Optom*. 2017;100(6):695-703. doi:10.1111/cxo.12527

30. Song AP, Yu T, Wang JR, Liu W, Sun Y, Ma SX. Multifocal electroretinogram in non-pathological myopic subjects: correlation with optical coherence tomography. *Int J Ophthalmol*. 2016;9(2):286-291. doi:10.18240/ijo.2016.02.21

31. Kawabata H, Adachi-Usami E. Multifocal electroretinogram in myopia. *Invest Ophthalmol Vis Sci*. 1997;38(13):2844-2851

32. Al-Haddad C, Bou Ghannam A, El Moussawi Z, et al. Multifocal electroretinography in amblyopia. *Graefes Arch Clin Exp Ophthalmol*. 2020;258(3):683-691. doi:10.1007/s00417-019- 04558-x

33. Palmowski-Wolfe A. Can the OCT replace functional tests such as the mfERG? *Invest Ophthalmol Vis Sci*. 2012;53(10):6129. doi:10.1167/iovs.12-10795

34. Divya Jagadeesh,Krupa Philip,Cathleen Fedtke, et al. Posterior segment conditions associated with myopia and high myopia. Clinical and Experimental Optometry. 2020;103 (6):756-765. doi:10.1111/cxo.13060

35. Guisela Fernández‐Espinosa,Elvira Orduna‐Hospital,Ana Boned‐Murillo, et al. Choroidal and Retinal Thicknesses in Type 2 Diabetes Mellitus with Moderate Diabetic Retinopathy Measured by Swept Source OCT. Biomedicines. 2022;10 (9):2314-2314. doi:10.3390/biomedicines10092314

36. Yang S, Zuo C, Xiao H, et al. Photoreceptor dysfunction in early and intermediate age-related macular degeneration assessed with mfERG and spectral domain OCT. Doc Ophthalmol. 2016;132(1):17-26. doi:10.1007/s10633-016-9523-4

37. Faghihi H, Hajizadeh F, Riazi-Esfahani M. Optical coherence tomographic findings in highly myopic eyes. J Ophthalmic Vis Res. 2010;5(2):110-121.
38. Yan Ni Yan,Ya Xing Wang,Liang Xu, et al. Fundus Tessellation: Prevalence and Associated Factors. Ophthalmology. 2015;122 (9):1873-1880. doi:10.1016/j.ophtha.2015.05.031
39. Hanyi Lyu,Qiuying Chen,Guangyi Hu, et al. Characteristics of Fundal Changes in Fundus Tessellation in Young Adults. Frontiers in Medicine. 2021;8 (0):0-0. doi:10.3389/fmed.2021.616249
40. Hood DC, Bach M, Brigell M, Keating D, Kondo M, Lyons JS, Palmowski-Wolfe AM. ISCEV standard for clinical multifocal electroretinography (mfERG) (2011 edition). Doc Ophthalmol. 2012;124(1):1-13. DOI:10.1007/s10633-011-9296-8
41.

Tables

Table. 1. Ocular biological parameters of the eyes in patients with fundus tessellation.

Variables	Grade 1（n=21）	Grade 2（n=20）	Grade 3（n=22）	Grade 4（n=24）	$F/H/\chi^2$	*P* value
Gender (Male/Female)	5/16	6/14	10/12	9/15	2.506	0.474
Age (years)	32.14±7.93	32.1±10.67	32.41±7.42	29.42±8.57	0.609	0.611
SE（D）	-7.30±1.04	-8.56±1.43[1)]	-8.76±1.96[1)]	-9.18±2.19[1)]	4.751	0.004
IOP (mmHg)	17.62±2.33	16.4±3.00	16.55±2.04	17.54±1.64	1.718	0.170
AL(mm)	25.95（25.34，27.58）	26.1(25.92，27.55）	27.28（26.82，28.1）	27.9（27.01，28.82）[1,2)]	13.819	0.003

Abbreviations: SE, Spherical equivalent; IOP, Intraocular pressure; AL, Axial length.

1) significant difference compared to Grade 1 group. 2) significant difference compared to Grade 2 group.

Table. 2. Comparison of the thickness of anatomicallayer, vascular density and MfERG of fundus tessellation.

	MT (μm)	RPE (μm)	SFCT (μm)	SVD (%)	DVD (%)	CFD (%)	N1 Amplitude (nV/deg^2)	P1 Amplitude (nV/deg^2)	N1 Latency(ms)	P1 Latency (ms)
Grade 1 (n=21)	196.95±11.71	21(20, 23)	205.07±27.5	35.34±4.82	22.56±3.27	33.62±4.55	40.26±5.45	69.65±8.53	24.36±1.01	41.99±0.8
Grade 2 (n=20)	196.73±14.95	22.5(20.63, 25.5)	170.6±28.33[1)]	33.67±4.09	20.39±2.98	33.68±3.23	34.21±3.05[1)]	64.76±8.17	25.21±3.47	42.71±2.63
Grade 3 (n=22)	206.78±23.44	20.5(19, 23.48)	155.25±34.64[1)]	28.33±7.52[12)]	20.63±3.55	33.09±4.51	29.87±4.95[12)]	58.74±7.39[1)]	26.35±3.7[1)]	43.71±2.09[1)]
Grade 4 (n=24)	199.58±17.43	21.75(19.25, 25.38)	127.02±40.45[123)]	34.78±5.81[3)]	22.30±4.21	32.52±4.73	27.71±6.46[12)]	52.36±14.57[123)]	27.14±2.1[12)]	44.38±1.92[12)]
F/H	1.544	2.625	20.994	6.839	2.096	0.351	24.865	11.885	4.326	6.415
P value	0.209	0.453	0.000	0.000	0.107	0.788	0.000	0.000	0.007	0.001

Abbreviations: MfERG, Multifocal visual electrophysiology: MT, Macular foveal thickness; SFCT, Subfoveal choroidal thickness; SVD, Superficial retinal capillary layer vascular density; DVD, Deep retinal capillary layer vascular density; CFD, Choroidal blood capillary layer blood flow density.

Note: 1): the difference is statistically significant compared to Grade 1. 2) :the difference is statistically significant compared to Grade 2. 3):the difference is statistically significant compared to Grade 3.

Table 3. Logistic regression analysis between variety parameters and fundus tessellation classification.

Variables	*β*	*S.E.*	*Wald value*	*p* value	*OR (95%CI)*
SFCT	-0.034	0.010	10.903	0.001	0.967（0.947，0.986）
N1 Amplitude	-0.407	0.120	11.498	0.001	0.666（0.526，0.842）
P1 Latency	0.465	0.172	7.281	0.007	1.592（1.136，2.231）

Abbreviations: SFCT, Subfoveal choroidal thickness.

Table 4. Pearson correlation analysis of SFCT with N1, P1 amplitude and latency time.

SFCT	*r*	*P*
N1 Amplitude	0.270	0.011
P1 Amplitude	0.246	0.022
N1 Latency	-0.219	0.041
P1 Latency	-0.248	0.021

Abbreviations: SFCT, Subfoveal choroidal thickness.

Table 5. Pearson correlation analysis of vascular density with N1, P1 amplitude and latency time.

	SVD		DVD		CFD	
	r	*P*	*r*	*P*	*r*	*P*
N1 Amplitude	0.022	0.841	0.000	0.996	-0.026	0.809
P1 Amplitude	-0.090	0.407	-0.104	0.337	-0.017	0.878
N1 Latency	0.146	0.177	0.135	0.213	0.008	0.942
P1 Latency	-0.099	0.363	-0.099	0.360	-0.087	0.422

Abbreviations: SVD, Superficial retinal capillary layer vascular density; DVD, Deep retinal capillary layer vascular density; CFD, Choroidal blood capillary layer blood flow density.

Table 6. ROC curve analysis of SFCT.

Group	Area	Standard Error	*p* value	95% Lower Limit	95% Upper Limit	Cutoff Value (μm)	Sensitivity	Specificity	Youden Index
Grade1-2	0.820	0.072	0.000	0.680	0.961	192.750	0.762	0.900	0.662
Grade2-3	0.695	0.084	0.030	0.531	0.860	162.000	0.7	0.682	0.382
Grade3-4	0.741	0.076	0.005	0.593	0.890	130.750	0.818	0.667	0.485

Abbreviations: ROC, Receiver-operating characteristic curve. SFCT, Subfoveal choroidal thickness.

Figures and legends.

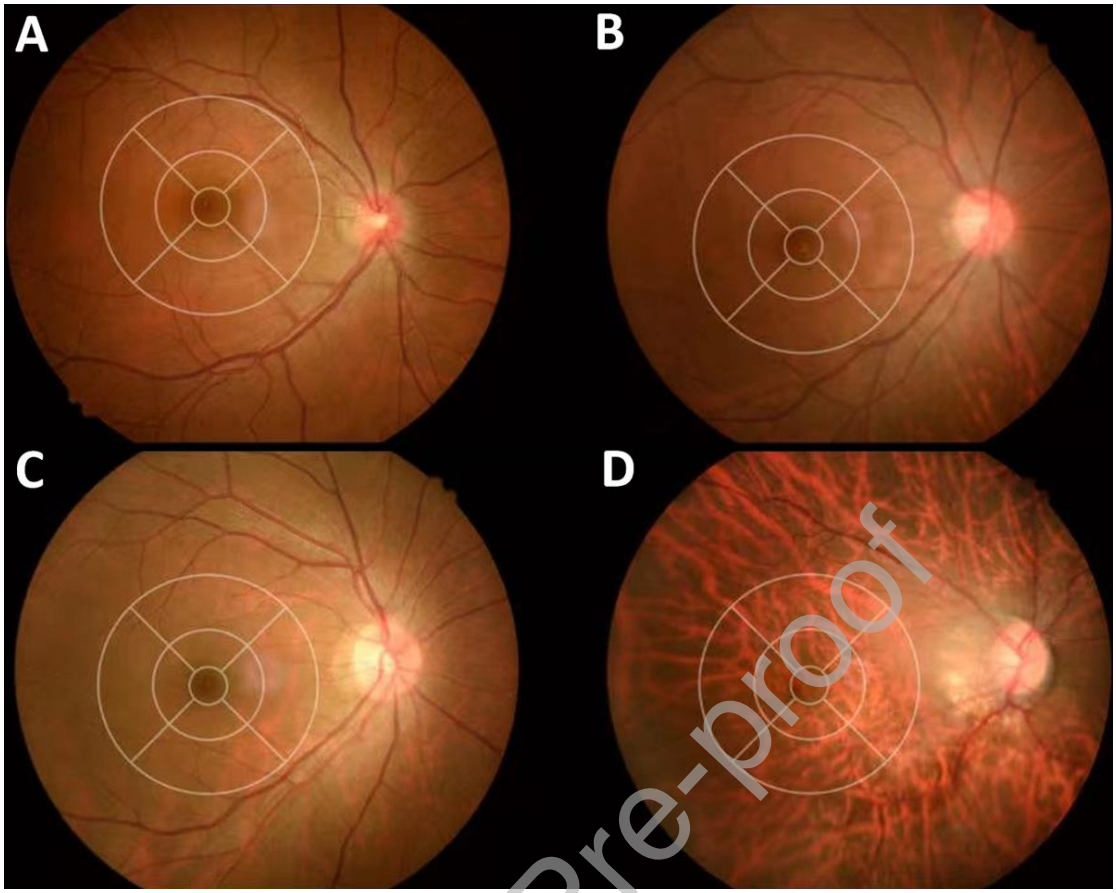

Figure 1. Schematic diagram of myopic fundus tessellation eyes grading. According to the ETDRS grid partition, the three circles are 1 mm, 3 mm and 6 mm from the center respectively. A:grade 1 as posterior extremely visible choroidal great vessels but not involving ETDRS grid, B:grade 2 as FT visible in the outer ring of ETDRS grid but not involving the middle ring, C:grade 3 as FT visible in the middle ring of ETDRS grid but not involving the inner macular fovea. D:grade 4 shows visible large choroidal vessels within the inner circle of the ETDRS grid at the fovea

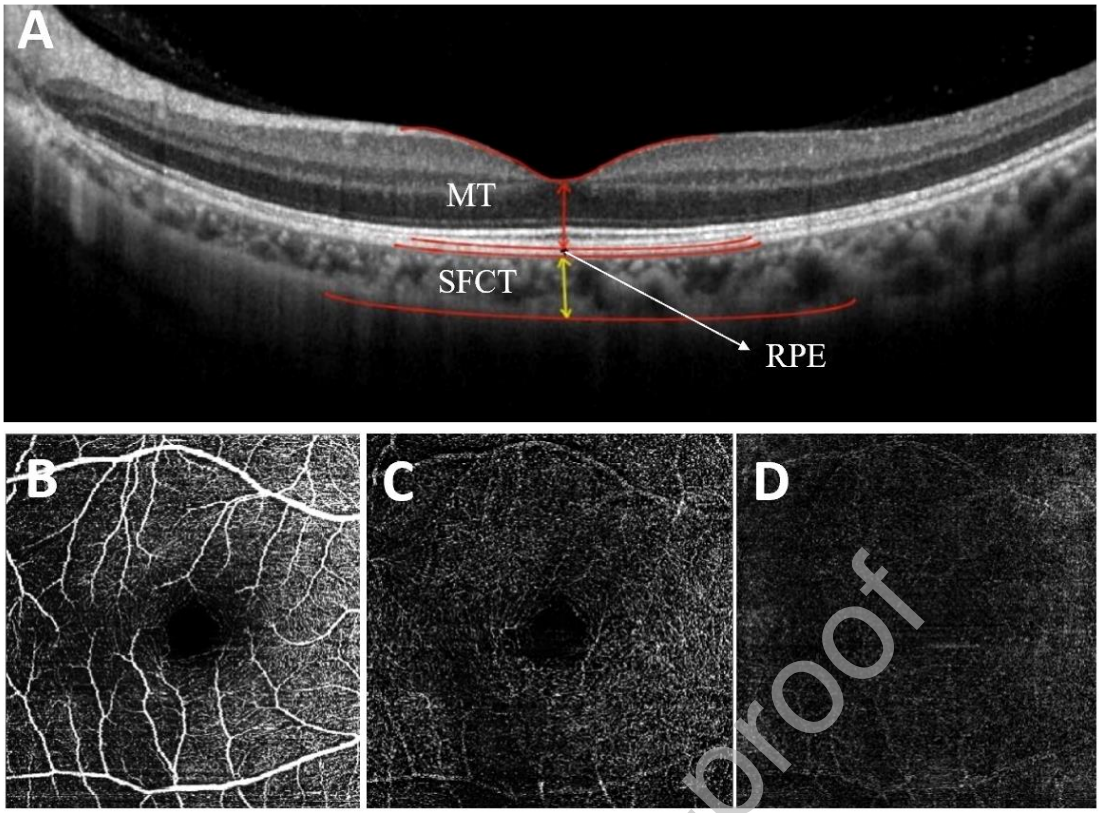

Figure 2. Diagram of the retinal layers obtained by EDI-OCT. OCT image of a patient with high myopia with FT(stage3) A: MT (Red arrows), RPE (Black arrows), SFCT (Yellow arrows). B: the superficial retinal capillary plexus. C: the deep retinal capillary plexus. D: the choroidal capillary plexus. Abbreviations: MT, Macular foveal thickness; SFCT, Subfoveal choroidal thickness; RPE, Retinal pigment epithelium.

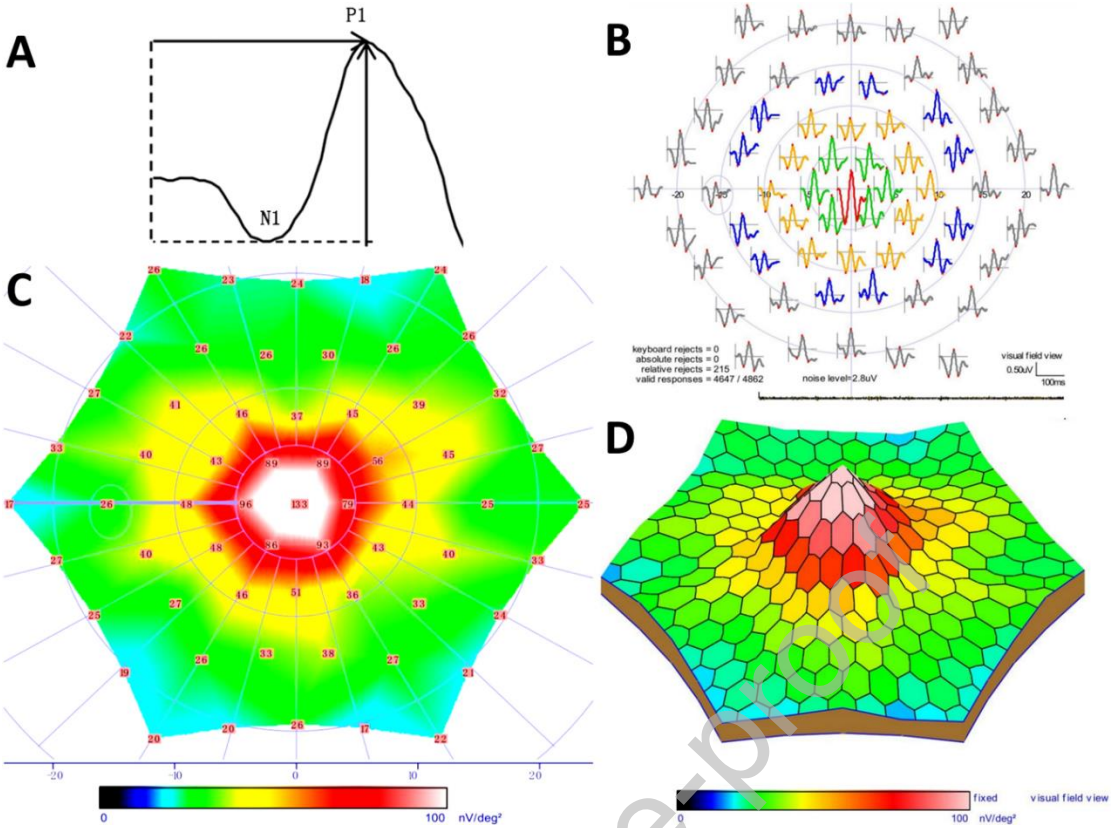

Figure 3. Main features of the basic multifocal electroretinogram waveform. A: The amplitude is the trough-to-peak amplitude (vertical arrow), and the horizontal arrow shows as latency (N for negative wave and P for positive wave). B: Ultifocal electroretinogram 61 hexagonal stimulus unit waveform arrays are grouped into 1~5 loops according to concentric loops (red represents loop 1, green represents loop 2, yellow represents loop 3, blue represents loop 4, and gray represents loop 5). C,D: Amplitude density of 61 hexagonal stimulus units in multifocal electroretinogram.

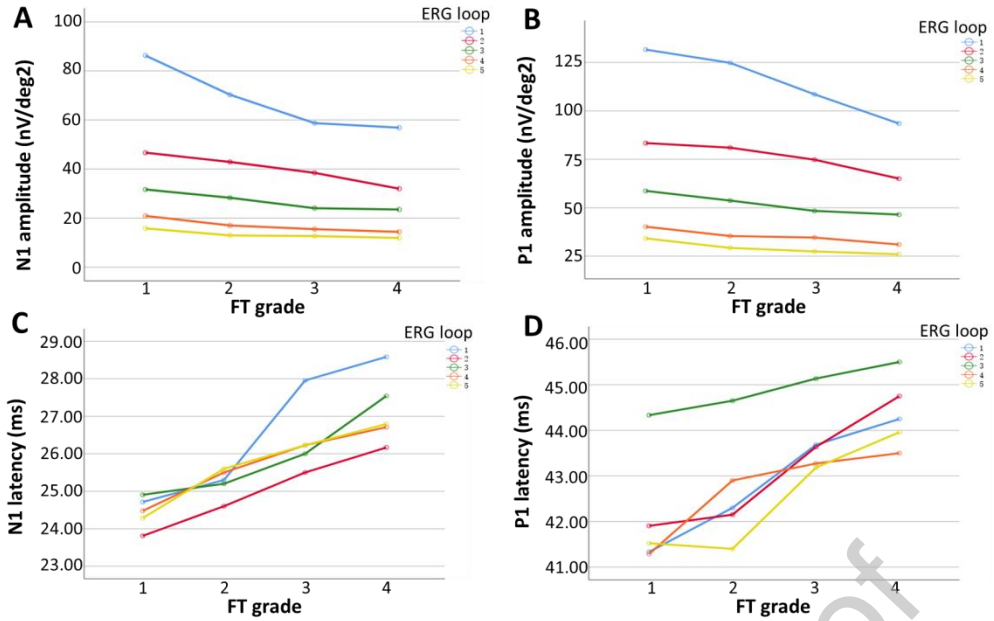

Figure 4. Folding line diagram show the amplitude (A, B) and latency (C, D) of N1 wave, P1 wave in each ring of different fundus tessellation grades. In MFERG, the stimulus units are divided into five rings from inner to outer based on their spatial distribution and different regions of the retina. Blue represents loop 1, rrdg represents loop 2, green represents loop 3, orange represents loop 4, and yellow represents loop 5.

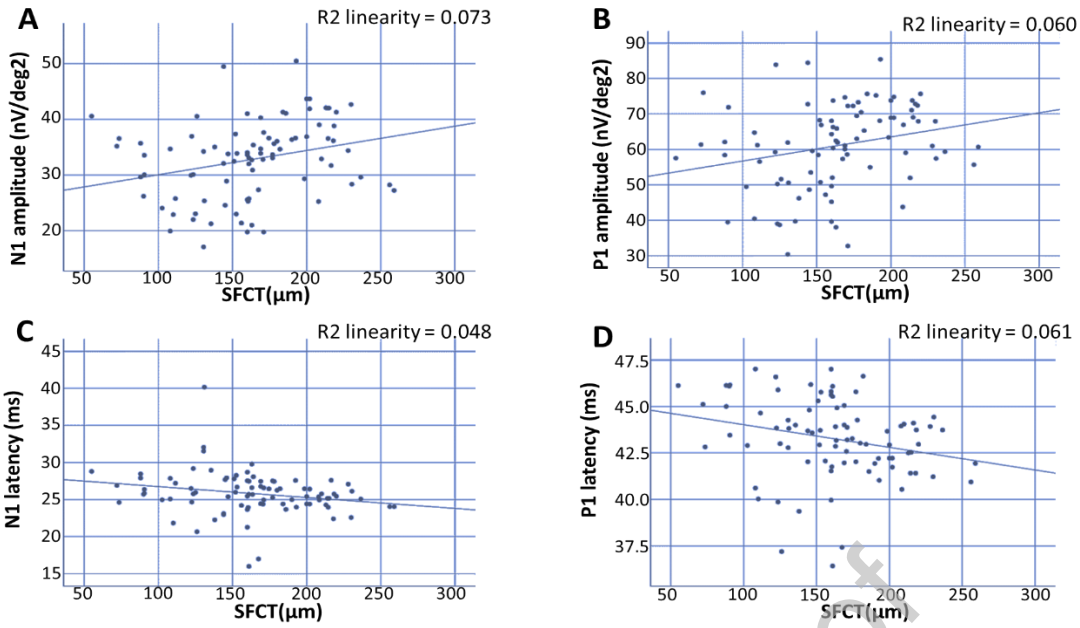

Figure 5. Correlation analysis of SFCT with N1, P1 amplitude and latency. A: The scatter plot of correlation between SFCT and N1 amplitude. B: The scatter plot of correlation between SFCT and P1 amplitude. C: The scatter plot of correlation between SFCT and N1 latency. D: The scatter plot of correlation between SFCT and P1 latency.

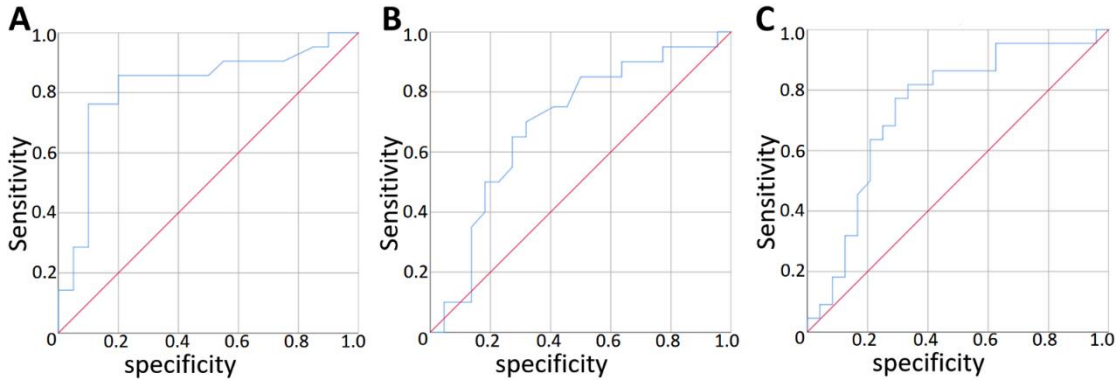

Figure 6. Area under the ROC curve (AUC) plot for each group of FT. A: ROC curves for FT eyes in the Grade 1 group versus SFCT in the Grade 2 group. B: ROC curves for FT eyes in the Grade 2 group versus SFCT in the Grade 3 group. C: ROC curves for FT eyes in the Grade 3 group versus SFCT in the Grade 4 group.

Funding:

This work was supported by Ningbo Medical Science and Technology Project (2021Y57), Ningbo Yinzhou District Agricultural Community Development Science and Technology Project (2022AS022). Ningbo Eye Hospital Science and Technology Project (2023YB004), Ningbo Eye Hospital Talent Project (2022RC001).**Availability of data and materials**

The datasets used and/ or analyzed during the present study are available from the corresponding author on reasonable request.

Ethics statement

The Medical Research Ethics Committee of Ningbo Eye Hospital (No. 2023022). **Competing interests**

This study did not receive any industrial support. The authors have no competing interests to declare regarding this study.